

Stretched Exponential Relaxation

D. C. Johnston

Ames Laboratory and Department of Physics and Astronomy, Iowa State University, Ames, Iowa 50011

(Dated: December 21, 2018)

Stretched exponential relaxation of a quantity n versus time t according to $n = n_0 \exp[-(\lambda^* t)^\beta]$ is ubiquitous in many research fields, where λ^* is a characteristic relaxation rate and the stretching exponent β is in the range $0 < \beta < 1$. Here we consider systems in which the stretched exponential relaxation arises from the global relaxation of a system containing independently exponentially relaxing species with a probability distribution $P(\lambda/\lambda^*, \beta)$ of relaxation rates λ . We study the properties of $P(\lambda/\lambda^*, \beta)$ and their dependence on β . Physical interpretations of λ^* and β , derived from consideration of $P(\lambda/\lambda^*, \beta)$ and its moments, are discussed.

I. INTRODUCTION

The stretched exponential relaxation function describes the time t dependence of a relaxing quantity n , according to

$$n = n_0 \exp[-(\lambda^* t)^\beta], \quad (1)$$

where $n_0 \equiv n(t = 0)$, λ^* is a characteristic relaxation rate, and the stretching exponent β is in the range $0 < \beta < 1$. This behavior has been observed for a wide variety of physical quantities in many different systems and research areas.¹ Log-linear and linear-log plots of the stretched exponential function versus $\lambda^* t$, which are the two most common ways of plotting the stretched exponential function, are shown in Figs. 1(a) and 1(b), respectively, for β values from 0.1 to 1 in 0.1 increments. All of the plots cross at a time $t_{1/e} = 1/\lambda^*$ at which the stretched exponential function has the value e^{-1} for all β . A pure exponential decay, corresponding to $\beta = 1$, plots as a straight line in Fig. 1(a). As β decreases from unity, more and more pronounced positive curvature is evident at small t . At small times, a Taylor series expansion of Eq. (1) for $\lambda^* t \ll 1$ gives

$$\frac{n}{n_0}(t \rightarrow 0) \approx 1 - (\lambda^* t)^\beta. \quad (2)$$

Thus the stretched exponential function with $0 < \beta < 1$ is singular at $t = 0$, with an infinitely negative slope there.

A natural and commonly used interpretation of an observed stretched exponential relaxation is in terms of the global relaxation of a system containing many independently relaxing species, each of which decays exponentially in time with a specific fixed relaxation rate λ . Then one can write the stretched exponential function as a sum of pure exponential decays, with a particular probability distribution P of λ values for a given value of β . In such a probability distribution, one must normalize λ to the characteristic relaxation rate λ^* appearing in the stretched exponential function (1). Hence for such systems one can write the stretched exponential function in Eq. (1) as

$$e^{-(\lambda^* t)^\beta} = \int_0^\infty P(s, \beta) e^{-s \lambda^* t} ds, \quad (3)$$

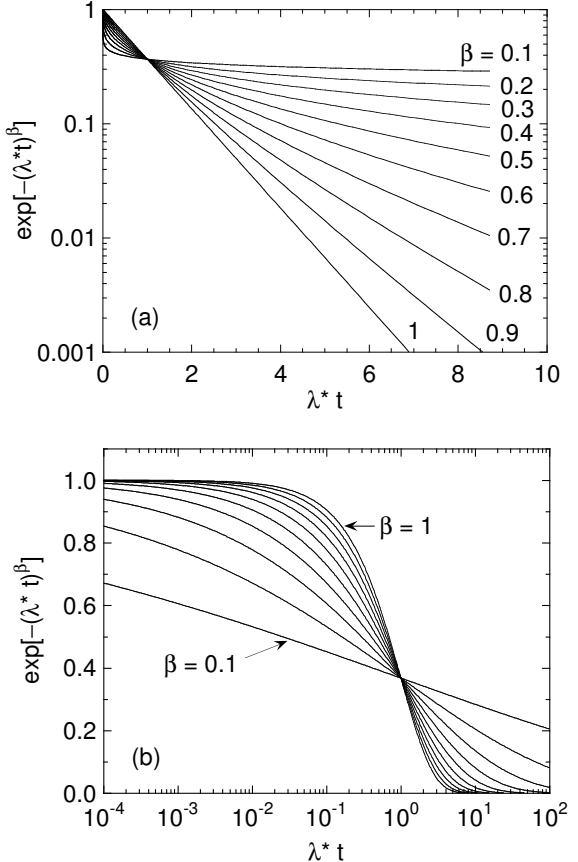


FIG. 1: Log-linear (a) and linear-log (b) plots of the stretched exponential function in Eq. (1) versus $\lambda^* t$ for β values from 0.1 to 1 in 0.1 increments.

where

$$s \equiv \frac{\lambda}{\lambda^*}.$$

Since $P(s, \beta)$ is a probability density, one has $\int_0^\infty P(s, \beta) ds = 1$.

A stretched exponential form of the ${}^7\text{Li}$ nuclear spin-lattice relaxation following saturation was recently observed^{2,3,4} in ${}^7\text{Li}$ NMR experiments on the heavy fermion⁵ compound LiV_2O_4 containing magnetic defects.⁴ In our attempts to understand the origin of

this non-exponential relaxation, we considered the above model of independently relaxing nuclear spins and found the published information on $P(s, \beta)$ (e.g., Refs. 6,7,8,9, 10,11,12,13) to be insufficient for our purposes, particularly with regard to the systematic behaviors of $P(s)$ versus β and to the physical significances of the parameters λ^* and β in the stretched exponential function (1). Since in the case of independently relaxing species the essential physics of the system resides in $P(s, \beta)$ rather than in the relaxation function (1) itself, we considered it important to further study $P(s, \beta)$. Here we report the results, some of which were briefly mentioned in Ref. 4.

II. RESULTS

A. The Probability Density

For $\beta = 1$, the stretched exponential function (1) is a pure exponential with relaxation rate $\lambda = \lambda^*$ and hence the probability density $P(s, 1)$ in Eq. (3) is a Dirac delta function at $s = 1$. For general β , from Eq. (3) one sees that $P(s, \beta)$ is the inverse Laplace transform of the stretched exponential, given by

$$P(s, \beta) = \frac{1}{2\pi i} \int_{-i\infty}^{i\infty} e^{-x^\beta} e^{sx} dx. \quad (4)$$

The change of variables $u = -ix$ allows one to write $P(s, \beta)$ as the Fourier transform

$$P(s, \beta) = \frac{1}{2\pi} \int_{-\infty}^{\infty} e^{-(iu)^\beta} e^{isu} du. \quad (5)$$

One can also express $P(s, \beta)$ as^{6,8,11}

$$P(s, \beta) = \frac{1}{\pi} \sum_{n=1}^{\infty} \frac{(-1)^{n+1} \Gamma(n\beta + 1)}{n! s^{n\beta+1}} \sin(n\pi\beta), \quad (6)$$

where $\Gamma(z)$ is the Gamma (factorial) function. Using Mathematica 4.0, we have obtained from Eqs. (5) and (6) closed analytic solutions for $P(s, \beta)$ for many rational values of β . The simplest expressions are obtained for $\beta = 1/3, 1/2$, and $2/3$, for which solutions have also been given in Refs. 9 and 10. For $\beta = 1/3$, we find the two alternative expressions

$$\begin{aligned} P\left(s, \frac{1}{3}\right) &= 3z^4 \text{Ai}(z) \\ &= \frac{1}{3\pi s^{3/2}} K_{1/3}\left(\frac{2}{\sqrt{27s}}\right), \end{aligned} \quad (7)$$

where $\text{Ai}(z)$ is the Airy function with $z = (3s)^{-1/3}$ and $K_n(x)$ is the modified Bessel function of the second kind. For $\beta = 1/2$, we get

$$P\left(s, \frac{1}{2}\right) = \frac{1}{\sqrt{4\pi s^3}} \exp\left(-\frac{1}{4s}\right), \quad (8)$$

which is also listed in tables of Laplace transforms.¹⁴ For $\beta = 2/3$, we obtain

$$P\left(s, \frac{2}{3}\right) = 6z^{7/4} \exp\left(-\frac{2}{27s^2}\right) [\text{Ai}(z) - \frac{1}{\sqrt{z}} \text{Ai}'(z)], \quad (9)$$

where $z = (3s)^{-4/3}$.

In general, the analytic results for rational $\beta = n/m$ values are expressed by Mathematica in terms of generalized hypergeometric functions ${}_pF_q(\mathbf{a}; \mathbf{b}; z)$. For example, for $\beta = 2/3$, $P(s, \beta)$ can also be expressed as

$$\begin{aligned} P\left(s, \frac{2}{3}\right) &= \frac{1}{\sqrt{3\pi s^{7/3}}} \left[s^{2/3} \Gamma\left(\frac{2}{3}\right) {}_1F_1\left(\frac{5}{6}, \frac{2}{3}, z\right) \right. \\ &\quad \left. + \Gamma\left(\frac{4}{3}\right) {}_1F_1\left(\frac{7}{6}, \frac{4}{3}, z\right) \right], \end{aligned} \quad (10)$$

with $z = -4/(27s^2)$. The expressions become progressively longer as the integer denominator m increases. For example, the expression for $P(s, \beta = 4/5)$ contains four additive ${}_pF_q(\mathbf{a}; \mathbf{b}; z)$ terms with $p = q = 3$ and $z = -256/(3125s^4)$, with $1/s^{1+n\beta}$ multiplicative prefactors where $n = 1$ to 4, respectively.

The probability density $P(s, \beta)$ in Eq. (3) is real by definition. By finding the real and imaginary parts of the integral on the right side of Eq. (5), one can explicitly show that the imaginary part is identically zero. The real part, which is $P(s, \beta)$, is found to be

$$P(s, \beta) = \frac{1}{\pi} \int_0^{\infty} e^{-u^\beta \cos(\pi\beta/2)} \cos[su - u^\beta \sin(\pi\beta/2)] du. \quad (11)$$

This integral can be evaluated numerically for arbitrary β using Mathematica. Similar expressions were obtained in Refs. 8 and 11.

The evolution of $P(s, \beta)$ versus s at fixed β for several rational values of β , from our analytic results, is plotted in Fig. 2(a) on linear scales and in Fig. 2(b) on semilog scales. The same type of plots as in Fig. 2(a) were previously given in Fig. 1 of Ref. 13, and related plots were given in Refs. 8 and 12. From Fig. 2(a), a $\beta < 1$ causes the infinitely high and narrow Dirac delta function probability distribution for $\beta = 1$ at $s = 1$ to broaden. $P(s)$ becomes highly asymmetric, and the peak in $P(s)$ becomes finite and moves towards slower rates which is compensated by a long tail to faster rates.

The value of s at which $P(s, \beta)$ is maximum for fixed β , $s(P^{\max})$, is plotted versus β on linear and semilog scales in Figs. 3(a) and (b), respectively. We find that $s(P^{\max})$ decreases with decreasing β and approaches zero exponentially for $\beta \lesssim 0.5$. A fit to the $s(P^{\max})$ versus β data in the range $1/8 \leq \beta \leq 1/2$ yielded

$$s(P^{\max}) \approx \frac{2.56}{\beta^{0.6}} \exp\left(-\frac{1.27}{\beta^{1.31}}\right). \quad (12)$$

Plots of this expression are shown as the solid curves in Figs. 3(a) and 3(b).

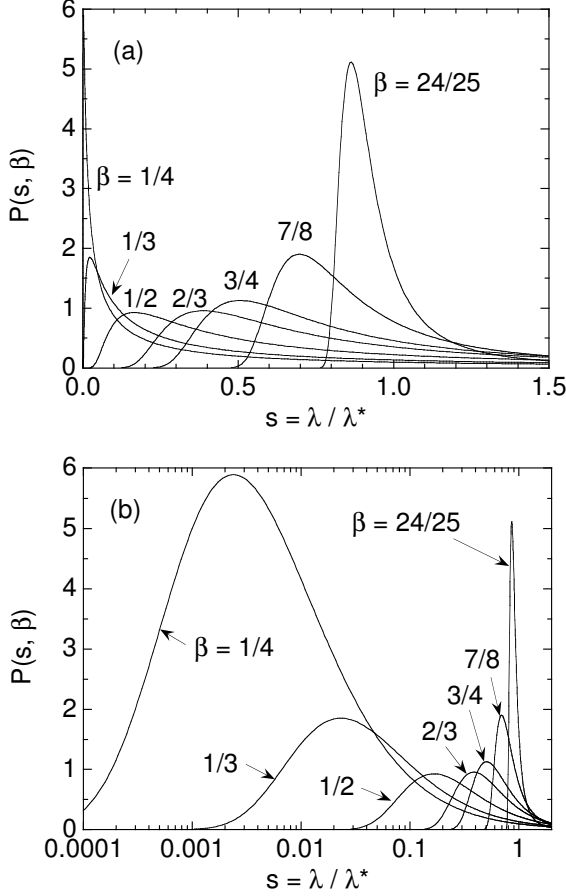


FIG. 2: Linear (a) and semilog (b) plots of the probability density $P(s, \beta)$ for the relaxation rate in Eq. (3) versus normalized relaxation rate $s = \lambda / \lambda^*$ for several rational values of β .

For small s , there is an exponential decrease in $P(s, \beta)$ with decreasing s that is given in the limit $s \rightarrow 0$ (i.e., below the peak) by^{9,11}

$$P(s \rightarrow 0, \beta) = \frac{a}{s^{1+\beta/[2(1-\beta)]}} \exp\left(-\frac{b}{s^{\beta/(1-\beta)}}\right). \quad (13)$$

where

$$a = \frac{\beta^{1+\beta/[2(1-\beta)]}}{\sqrt{2\pi\beta(1-\beta)}}$$

and

$$b = (1-\beta)\beta^{\beta/(1-\beta)}.$$

From Eq. (8) for $\beta = 1/2$ one gets directly that $a = 1/\sqrt{4\pi}$ and $b = 1/4$, in agreement with these results. Thus the probability distribution $P(s, \beta)$ contains an intrinsic low- s cutoff that decreases with decreasing β . Note that the peak position of $P(s, \beta)$ in Eq. (12) has the same form as the $s \rightarrow 0$ behavior in Eq. (13). We take the value of the low- s cutoff to be the position of the

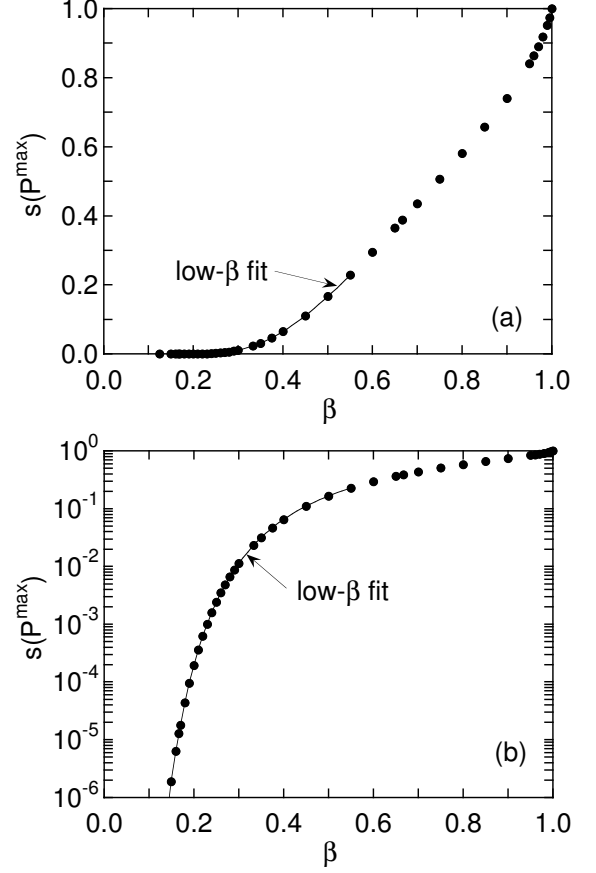


FIG. 3: Linear (a) and semilog (b) plots of the value $s(P^{\max})$ of s at which the probability density $P(s)$ in Eq. (3) (see Fig. 2) is maximum, plotted versus the stretching exponent β . The solid curve in (a) and (b) is an exponential fit to the data for $\beta \leq 0.5$ as given in Eq. (12). The position of the peak can be taken to be the intrinsic small- s cutoff to $P(s)$ (see text).

peak in $P(s, \beta)$ that is plotted in Fig. 3 and described by Eq. (12) for $\beta \lesssim 1/2$.

In the opposite limit of large $s \gg 1$, in Eq. (6) one retains only the first term in the power series, giving

$$P(s \rightarrow \infty, \beta) = \frac{c}{s^{1+\beta}}, \quad (14)$$

where

$$c = \frac{\Gamma(\beta + 1)}{\pi} \sin(\pi\beta). \quad (15)$$

For $0 < \beta < 1$, one has that $\Gamma(\beta + 1) \sim 1$.

The median s_{median} of the probability distribution $P(s)$ has not been discussed before in the literature to our knowledge. It is defined to be the value of s for which it is equally likely for s to be less than s_{median} as it is to be greater. It is calculated by solving the expression $\int_0^{s_{\text{median}}} P(s, \beta) ds = 1/2$ for a fixed value of β . The s_{median} is plotted versus β in Fig. 4(a), and an expanded plot of the data for $0.3 \leq \beta \leq 1$ is shown in Fig. 4(b). One sees from Fig. 4 that with decreasing β , s_{median} remains nearly equal to unity from $\beta = 1$

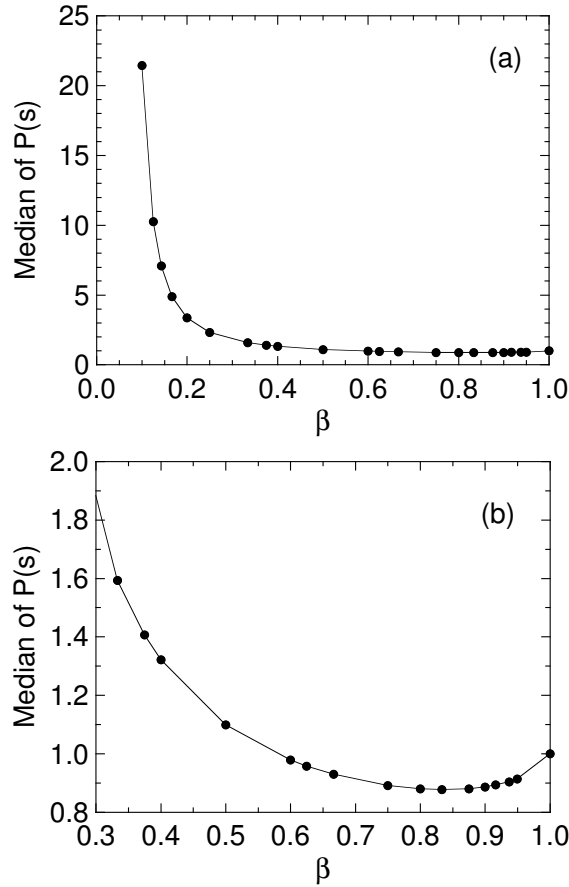


FIG. 4: (a) Median of the probability distribution $P(s)$ versus β . (b) Expanded plot of the data in (a) for $0.3 \leq \beta \leq 1$. The lines are guides to the eye.

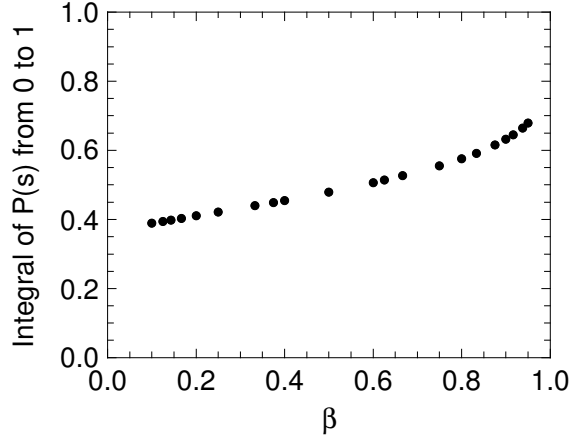


FIG. 5: The integral $\int_0^1 P(s, \beta) ds$ versus β .

down to about $\beta = 0.5$, below which s_{median} begins to increase dramatically. A related quantity is the integral $\int_0^1 P(s, \beta) ds$, which measures the probability that s is less than or equal to unity. If the median is at $s = 1$, then the integral should equal 1/2. The integral is plotted versus β in Fig. 5. In the range $0.1 \leq \beta \leq 0.9$, the

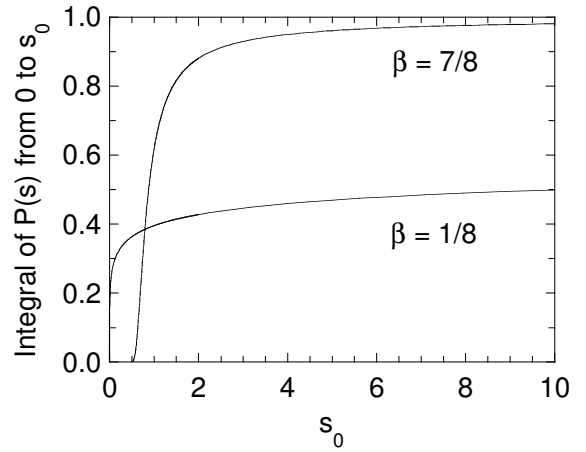


FIG. 6: Probability that s is less than the value s_0 , given by the integral $\int_0^{s_0} P(s, \beta) ds$, for $\beta = 1/8$ and $7/8$.

integral is equal to 1/2 to within ± 0.1 . The reason for the difference between the β dependences of the two quantities is apparent from plots for $\beta = 1/8$ and $7/8$ in Fig. 6 of the probability that s is less than a value s_0 , given by the integral $\int_0^{s_0} P(s, \beta) ds$. One sees from the figure how it happens that for $\beta = 1/8$, $s_{\text{median}} > \int_0^1 P(s, \beta) ds$, whereas for $\beta = 7/8$, $s_{\text{median}} \lesssim \int_0^1 P(s, \beta) ds$.

B. The Moments of $P(s, \beta)$

The moments of the probability distribution are defined by $(s^n)_{\text{ave}} = \int_0^\infty s^n P(s, \beta) ds$. From Eq. (14), the $n = 1$ moment, which is the average $s_{\text{ave}} = (\lambda/\lambda^*)_{\text{ave}} = \lambda_{\text{ave}}/\lambda^*$, is infinite for all β with $0 < \beta < 1$. Hence the average relaxation rate λ_{ave} is infinite. Indeed all positive moments such as also $(s^2)_{\text{ave}}$ are infinite. Very fast (infinite) relaxation rate components are required to produce the infinitely negative slope for any $\beta < 1$ in the stretched exponential function (1) as $t \rightarrow 0$ as described in Eq. (2) and seen in Fig. 1(a). A cutoff to $P(s, \beta)$ at large s is required to obtain a finite initial slope of $n(t)$ in Eq. (1) and finite averages $(s^n)_{\text{ave}}$. Every real system must have a high- s cutoff to $P(s, \beta)$, but of course it will depend on the system under consideration. We will return to this issue in Sec. II D.

On the other hand, the $n = -1$ moment of $P(s, \beta)$, which is the average $(1/s)_{\text{ave}} = (\lambda^*/\lambda)_{\text{ave}}$, is finite for $0 < \beta \leq 1$ and increases monotonically and rapidly with decreasing β , diverging at $\beta = 0$. In general, one has⁸

$$\left[\left(\frac{\lambda^*}{\lambda} \right)^m \right]_{\text{ave}} = \frac{\Gamma(m/\beta)}{\beta \Gamma(m)}, \quad (16)$$

where $m = -n$. A semilog plot of $(\lambda^*/\lambda)_{\text{ave}}$ versus β for $0.01 \leq \beta \leq 1$ is shown in Fig. 7.

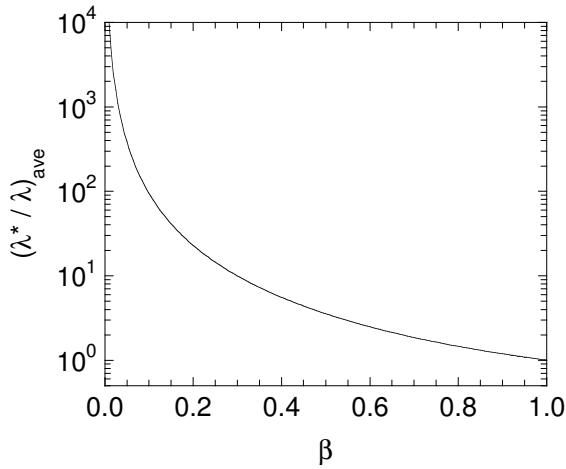


FIG. 7: Semilog plot of the average $(\lambda^*/\lambda)_{\text{ave}}$ versus the stretching exponent β according to Eq. (16) with $m = 1$.

C. Physical Interpretations of λ^* and β

The parameter λ^* in the stretched exponential function (1) is often referred to in the literature as some undefined “characteristic relaxation rate” or as some undefined “average” relaxation rate. As shown above, λ^* is neither the average of λ [which is infinite in the absence of a high- s cutoff to $P(s, \beta)$] nor the inverse of the average of $1/\lambda$. Evidently λ^* is a characteristic property of $P(s, \beta)$ itself and not of its moments. Indeed, from the above discussion and the data in Fig. 5, we infer that the physical interpretation of λ^* is that λ is about equally likely to be less than λ^* as it is to be greater (to within $\sim \pm 20\%$). From Fig. 4, one sees that λ^* is within about 10% of the median of $P(s, \beta)$ for $0.5 \leq \beta \leq 1$. For $\beta < 0.5$, the median strongly increases due to the long high- s tail to $P(s, \beta)$, but the integral in Fig. 5 continues to decrease slowly with decreasing β .

The stretching exponent β is often cited as a measure of the width Δs of the distribution $P(s, \beta)$. However, a statistical definition of the width such as the rms width $\Delta s = \sqrt{(s^2)_{\text{ave}} - (s_{\text{ave}})^2}$ is undefined for $P(s, \beta)$ since as shown above both of the averages in the square root are infinite in the absence of a high- s cutoff to $P(s, \beta)$. Another possibility is that β is a measure of the full width at half maximum ($\Delta s \equiv \text{FWHM}$) of $P(s, \beta)$. From Fig. 8(a), the FWHM initially increases as β decreases below unity, but then decreases as β decreases further for $\beta \lesssim 0.65$. Therefore, β is a multivalued function of FWHM, and hence correlation with the FWHM is not a useful physical interpretation of β . On a logarithmic s scale, the FWHM increases monotonically with decreasing β as shown in Fig. 8(b), and appears to diverge as $\beta \rightarrow 0$. Therefore β can be considered to be related to the *logarithmic* FWHM of $P(s)$, but not to the FWHM itself.

Therefore we seek a physical interpretation of β that is not explicitly tied to the width of $P(s, \beta)$ versus s . We have seen above that the position $s(P^{\max})$ of the peak

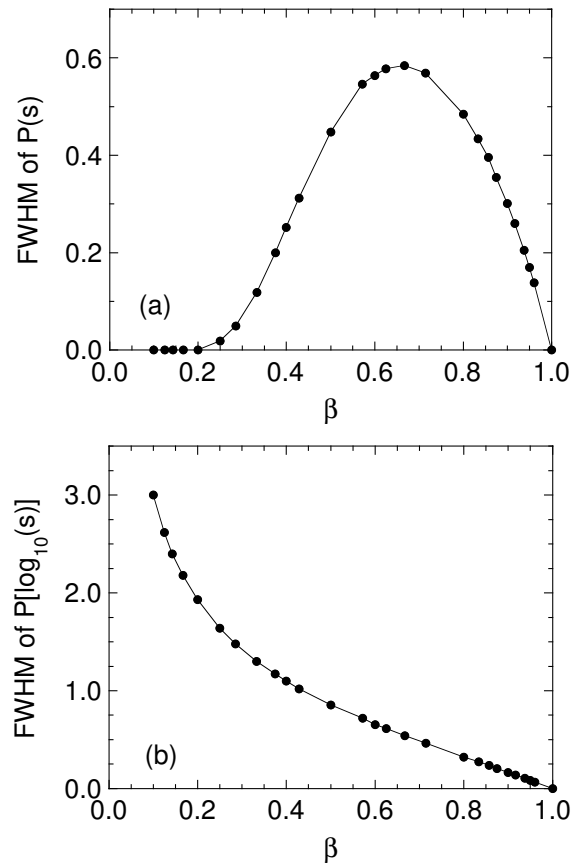


FIG. 8: Full width at half maximum peak value (FWHM) versus β of the probability distribution $P(s)$ on a linear s scale (a) and of $P(\log_{10}(s))$ on a logarithmic s scale (b). See Figs. 2(a) and (b), respectively. The solid curves are guides to the eye.

in $P(s, \beta)$, plotted in Fig. 3 versus β , decreases monotonically with decreasing β , and that below the peak, $P(s, \beta)$ decreases exponentially as s decreases. As discussed above, this demonstrates that $P(s, \beta)$ has a low- s cutoff that decreases monotonically with decreasing β . Thus a useful physical interpretation of β is that β is a measure of the intrinsic small-relaxation-rate cutoff of $P(s, \beta)$. To our knowledge, this identification and the above physical interpretation of λ^* here and in Ref. 4 have not appeared elsewhere in the literature.

One can rewrite the stretched exponential function (1) as

$$n = n_0 \exp[-(t/\tau^*)^\beta], \quad (17)$$

where the relaxation time of a particular relaxing species in the system is $\tau = 1/\lambda$ and the characteristic relaxation time of the probability distribution is $\tau^* = 1/\lambda^*$, so $\tau/\tau^* = \lambda^*/\lambda$. From the above results, one obtains, for example, that the plot of $(\lambda^*/\lambda)_{\text{ave}}$ versus β in Fig. 7 is the same as a plot of τ_{ave}/τ^* versus β . From Fig. 7, the normalized average relaxation time τ_{ave}/τ^* is well-defined at each β , increases monotonically and rapidly as

β decreases below unity, and diverges as $\beta \rightarrow 0$. Thus an additional physical interpretation of β is that $1/\beta$ is a measure of the average relaxation time of the relaxing species in the system relative to the parameter $\tau^* = 1/\lambda^*$.

D. Influences of a Large- s Cutoff to $P(s, \beta)$

We have alluded above to the singular nature of the stretched exponential function (1) at time $t = 0$. Associated with this singularity are infinite averages $(s^n)_{\text{ave}}$ with positive integer n for any fixed β with $0 < \beta < 1$. Here we briefly discuss the influences of a large- s cutoff s_{cutoff} to $P(s, \beta)$ on s_{ave} and on the relaxation function that can be computed from the modified $P(s, \beta, s_{\text{cutoff}})$. That relaxation function is no longer a pure stretched exponential. By definition, then,

$$P(s, \beta, s_{\text{cutoff}}) = 0 \quad \text{for } s \geq s_{\text{cutoff}}. \quad (18)$$

For illustrative purposes, we consider the probability distribution for $\beta = 1/2$ because of the simple form of $P(s, \beta = 1/2)$ in Eq. (8). This β value is also commonly observed in real systems so the discussion here may have practical applications. The only influence of the cutoff on $P(s, \beta)$, beyond the cutoff condition (18), is that $P(s, \beta)$ must be renormalized so that

$$\int_0^{s_{\text{cutoff}}} P(s, \beta, s_{\text{cutoff}}) ds = 1. \quad (19)$$

Applying conditions (18) and (19) to $P(s, 1/2)$ in Eq. (8) gives, for $s \leq s_{\text{cutoff}}$,

$$P(s, 1/2, s_{\text{cutoff}}) = \frac{\exp(-\frac{1}{4s})}{\sqrt{4\pi s^3} \operatorname{erfc}(\frac{1}{2\sqrt{s_{\text{cutoff}}}})}, \quad (20)$$

where $\operatorname{erfc}(z)$ is the complementary error function.

The average of s is $s_{\text{ave}} = \int_0^{s_{\text{cutoff}}} s P(s, \beta, s_{\text{cutoff}}) ds$, yielding for $\beta = 1/2$

$$s_{\text{ave}} = \frac{\sqrt{s_{\text{cutoff}}} \exp(-\frac{1}{4s_{\text{cutoff}}})}{\sqrt{\pi} \operatorname{erfc}(\frac{1}{2\sqrt{s_{\text{cutoff}}}})}. \quad (21)$$

Linear and log-log plots of s_{ave} versus s_{cutoff} are shown in Figs. 9(a) and 9(b), respectively. For $s_{\text{cutoff}} \gg 1$, one can approximate Eq. (21) as

$$s_{\text{ave}} = \frac{1}{\pi} - \frac{1}{2} + \sqrt{\frac{s_{\text{cutoff}}}{\pi}} \quad (s_{\text{cutoff}} \gg 1).$$

From Eq. (3), one obtains the time dependence of the relaxation of the quantity $n(t)$ using

$$\frac{n(t)}{n_0} = \int_0^\infty P(s, \beta) e^{-s\lambda^* t} ds, \quad (22)$$

or, with a cutoff present,

$$\frac{n(t)}{n_0} = \int_0^{s_{\text{cutoff}}} P(s, \beta, s_{\text{cutoff}}) e^{-s\lambda^* t} ds. \quad (23)$$

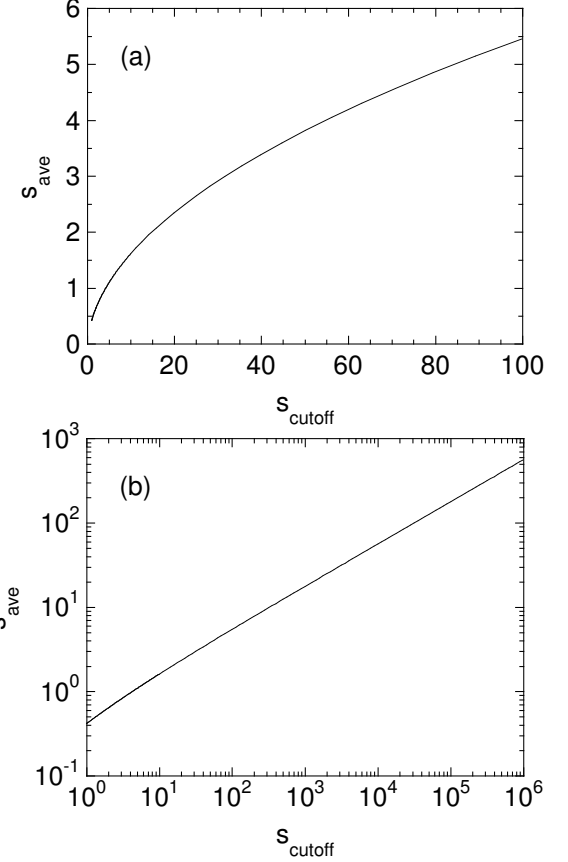


FIG. 9: Linear (a) and log-log (b) plots of $s_{\text{ave}} = \lambda_{\text{ave}}/\lambda^*$ in Eq. (21) versus the large- s cutoff s_{cutoff} to the probability distribution $P(s, \beta = 1/2, s_{\text{cutoff}})$ in Eq. (20).

Shown in Fig. 10(a) are plots of n/n_0 versus t for $\beta = 1/2$ and for $s_{\text{cutoff}} = 100$ and ∞ , where $P(s, 1/2, s_{\text{cutoff}})$ is given in Eq. (20). Expanded plots for $\lambda^* t \ll 1$ are shown in Fig. 10(b). If there is no large- s cutoff, then $s_{\text{ave}} = \infty$ and the initial slope of n/n_0 versus t is $-\infty$ for $0 < \beta < 1$ as previously discussed. However, the presence of the cutoff gives a finite s_{ave} and an initial linear decrease of $n(t)/n_0$ versus time as seen in Fig. 10(b). In that case, at sufficiently small $t \ll (s_{\text{cutoff}}\lambda^*)^{-1}$ one can Taylor expand the exponential in Eq. (23) to get $e^{-s\lambda^* t} \approx 1 - s\lambda^* t$. Substituting this expression for the exponential into Eq. (23) gives

$$\frac{n(t \rightarrow 0)}{n_0} = 1 - s_{\text{ave}}\lambda^* t = 1 - \lambda_{\text{ave}} t,$$

where we have used $s_{\text{ave}} = \lambda_{\text{ave}}/\lambda^*$. The initial slope of n/n_0 versus t is then a true measure of the negative of the average relaxation rate λ_{ave} in the system. Every real system must have a large- s cutoff. Experimentally, an important resolution issue is being able to look at short enough times to be confident that one is measuring the initial slope of the relaxation. The length of time that the initial linear relaxation is retained increases as s_{cutoff} decreases.

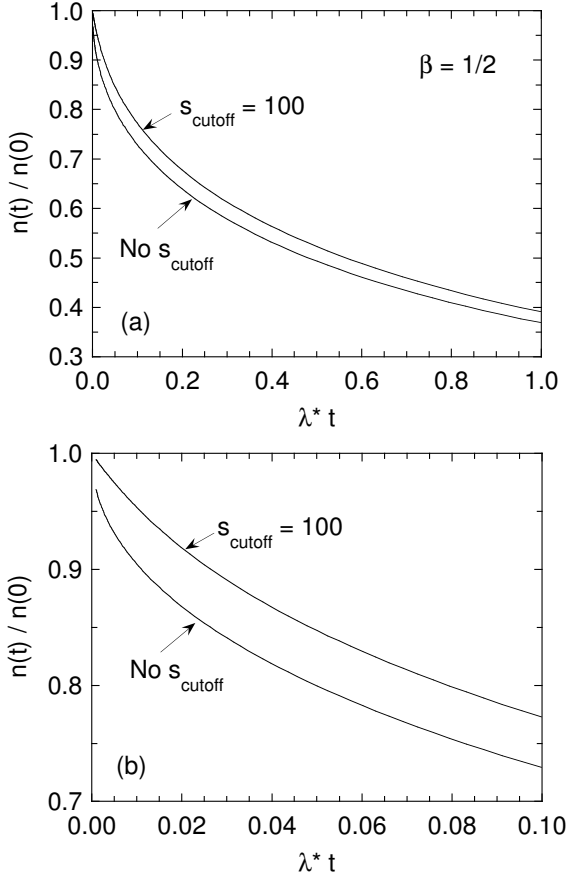


FIG. 10: (a) Comparison of the time t dependent stretched exponential relaxation with $\beta = 1/2$ without a cutoff to the probability distribution and with a cutoff $s_{\text{cutoff}} = 100$. (b) Expanded plot of the data in (a) near $t = 0$. Note the initial linear dependence of n on t with the finite cutoff $s_{\text{cutoff}} = 100$.

III. SUMMARY

The ubiquitous stretched exponential relaxation function (1) has been found to apply to the relaxation behavior of many different systems. In this paper we have examined some systematics of the probability distribution $P(s, \beta)$, where $s = \lambda/\lambda^*$, that apply in the particular case that the stretched exponential function arises from the global sum of exponential decays of independently relaxing species with relaxation rates λ .

The functional dependence of the peak position of $P(s)$ on β has been determined. This peak position decreases

monotonically with decreasing β and was characterized as a measure of the intrinsic low- s cutoff possessed by $P(s)$. We therefore suggested that a physical interpretation of β is that β is a measure of this intrinsic low- s cutoff. Additionally, $1/\beta$ is a measure of the average relaxation time (not rate) of the relaxing constituents of the system. These interpretations contrast with a common one that β is a measure of the width in s of $P(s, \beta)$ which was shown to be not quantitatively useful.

We derived and discussed the β -dependence of the median of $P(s)$. The positive moments of $P(s)$, which are the averages $(s^n)_{\text{ave}}$, are infinite in the absence of a large- s cutoff to $P(s, \beta)$, so λ^* is not related to any such average as often assumed. We suggested instead that the fundamental physical interpretation of λ^* is that λ is about equally likely (to within $\sim \pm 20\%$) to be less than λ^* as it is to be greater.

The influence of a large- s cutoff to $P(s, \beta)$ on $s_{\text{ave}} = \lambda_{\text{ave}}/\lambda^*$ and on the time dependence of the relaxation were investigated for the illustrative case of $\beta = 1/2$. The cutoff leads to a finite average relaxation rate that decreases as the cutoff decreases. The cutoff also removes the infinite-slope singularity in the stretched exponential relaxation at time $t = 0$ and replaces it with an initial linear time dependence, the slope of which is the negative of the average relaxation rate of the constituent relaxing species in the system.

We note that experimental time-dependent relaxation data can often be fitted by a discrete sum of exponential relaxations, as well as by the stretched exponential function. Thus experimental resolution is important to distinguishing between such similar types of fits. Ultimately, the justification for using the stretched exponential function to fit relaxation data, as opposed to some other function such as a discrete sum of decaying exponentials, must reside in the physics of the system under consideration.

Acknowledgments

The author is grateful for the collaboration of and discussions with his coauthors of Ref. 4. Ames Laboratory is operated for the U.S. Department of Energy by Iowa State University under Contract No. W-7405-Eng-82. This work was supported by the Director for Energy Research, Office of Basic Energy Sciences.

¹ J. C. Phillips, Rep. Prog. Phys. **59**, 1133 (1996).

² W. Trinkl, N. Büttgen, H. Kaps, A. Loidl, M. Klemm, and S. Horn, Phys. Rev. B **62**, 1793 (2000).

³ H. Kaps, M. Brando, W. Trinkl, N. Büttgen, A. Loidl, E.-W. Scheidt, M. Klemm, and S. Horn, J. Phys.: Condens. Matter **13**, 8497 (2001).

⁴ D. C. Johnston, S.-H. Baek, X. Zong, F. Borsa, J. Schmalian, and S. Kondo, Phys. Rev. Lett. **95**, 176408 (2005).

⁵ S. Kondo, D. C. Johnston, C. A. Swenson, F. Borsa, A. V. Mahajan, L. L. Miller, T. Gu, A. I. Goldman, M. B. Maple, D. A. Gajewski, E. J. Freeman, N. R. Dilley, R. P.

Dickey, J. Merrin, K. Kojima, G. M. Luke, Y. J. Uemura, O. Chmaissem, and J. D. Jorgensen, *Phys. Rev. Lett.* **78**, 3729 (1997).

⁶ H. Pollard, *Bull. Am. Math. Soc.* **52**, 908 (1946).

⁷ G. Williams and D. C. Watts, *Trans. Faraday Soc.* **66**, 80 (1970).

⁸ C. P. Lindsey and G. D. Patterson, *J. Chem. Phys.* **73**, 3348 (1980).

⁹ E. Helfand, *J. Chem. Phys.* **78**, 1931 (1983).

¹⁰ E. W. Montroll and J. T. Bendler, *J. Stat. Phys.* **34**, 129 (1984).

¹¹ K. Weron, *Acta Phys. Pol. A* **70**, 529 (1986).

¹² I. Svare, S. W. Martin, and F. Borsa, *Phys. Rev. B* **61**, 228 (2000).

¹³ P. Hetman, B. Szabat, K. Weron, and D. Wodziński, *J. Non-Cryst. Solids* **330**, 66 (2003).

¹⁴ M. Abramowitz and I. A. Stegun, *Handbook of Mathematical Functions* (Dover, New York, 1972), Eq. 29.3.82.